All-optical wavelength conversion at bit rates above 10 Gb/s using semiconductor optical amplifiers

Jørgensen, Carsten; Danielsen, Søren Lykke; Stubkjær, Kristian; Schilling, M.; Daub, K.; Doussiere, P.; Pommerau, F.; Hansen, Peter Bukhave; Poulsen, Henrik Nørskov; Kloch, Allan

Total number of authors:
16

Published in:
I E E E Journal on Selected Topics in Quantum Electronics

Link to article, DOI:
10.1109/2944.658592

Publication date:
1997

Document Version
Publisher's PDF, also known as Version of record

All-Optical Wavelength Conversion at Bit Rates Above 10 Gb/s Using Semiconductor Optical Amplifiers

C. Joergensen, S. L. Danielsen, K. E. Stubkjaer, *Member, IEEE,* M. Schilling, *Member, IEEE,* K. Daub, P. Doussiere, F. Pommerau, P. B. Hansen, H. N. Poulsen, A. Kloch, M. Vaa, B. Mikkelsen, E. Lach, G. Laube, W. Idler, and K. Wunstel

(Invited Paper)

***Abstract*—This work assesses the prospects for high-speed all-optical wavelength conversion using the simple optical interaction with the gain in semiconductor optical amplifiers (SOA's) via the interband carrier recombination. Operation and design guidelines for conversion speeds above 10 Gb/s are described and the various tradeoffs are discussed. Experiments at bit rates up to 40 Gb/s are presented for both cross-gain modulation (XGM) and cross-phase modulation (XPM) in SOA's demonstrating the high-speed capability of these techniques.**

***Index Terms*—Optical amplifiers, optical communication, optical frequency conversion, optical signal processing, wavelength-division multiplexing.**

I. Introduction

SEVERAL FIELD trials with wavelength-division multiplexed (WDM) networks that feature wavelength switching and routing are now planned or in progress, e.g., [1]–[3]. Although the investigations of WDM network architectures are only at their beginning, it seems that for full flexibility it is very attractive to be able to translate the channel wavelengths in an easy way [4], [5]. Work on different wavelength conversion principles are, therefore, getting considerable attention. The plain solution to wavelength conversion is use of optoelectronic conversion combined with electronic repeaters or regenerators. Wavelength conversion based on this principle has recently been demonstrated in a three node network with four WDM-channels each at 2.5 Gb/s [6]. The optoelectronic converters have low optical power requirements and potentially a large input power dynamic range. However, for wavelength conversion in high-speed networks operating at 10 Gb/s and in the future possibly at 100 Gb/s, the power consumption of the optoelectronic converter will be high and limitations of electronic circuitry may be encountered. Therefore, all-optical converters are highly interesting. Promising techniques relying on four-wave mixing (FWM) in fibers and semiconductor optical amplifiers (SOA's) [7]–[10], optical modulation of lasers [11]–[19], cross-gain modulation (XGM) and cross-phase modulation (XPM) in SOA's [20]–[37] have been reported. Difference frequency generation in periodic waveguide structures of $LiNbO_3$ [38] or AlGaAs [39] has also been investigated.

For intensity modulated (IM) systems the most practical all-optical converters with polarization independent operation and high-quality converted signals seem to be devices using XGM or XPM in SOA's. The XGM and XPM schemes feature high conversion efficiencies as well as insensitivity to the signal polarization. The conversion speed is determined by the carrier dynamics that for both converter types are governed by the relative slow interband carrier recombinations [40]. An important task for the next generation of these converters is to achieve fast carrier dynamics to enable efficient high-speed wavelength converters that can operate above 40 Gb/s. So far, XGM and XPM wavelength conversion with low penalty have been achieved at 20 Gb/s [28], [29], [41], and recently also at 40 Gb/s using speed optimized SOA's [30], [42].

The widely studied FWM in SOA's is inherently fast since it exploits the ultra fast intraband carrier recombination processes with life times in the picosecond range [43]. These converters can handle all signal modulation formats in contrast to the XGM and XPM converters that only allow IM input signals. Unfortunately, FWM suffers from a poor efficiency and requires tight optical filtering at the output of the wavelength converters for a good signal-to-noise ratio (SNR). Moreover, the FWM process has the disadvantage of being intrinsically polarization sensitive so two orthogonally polarized pump sources are needed for polarization insensitive operation.

In this paper, the focus is therefore on the recent work toward high-speed SOA converters using XGM and XPM. Section II presents experimental and theoretical studies of the optical modulation bandwidth of SOA's and gives guidelines on how to increase the conversion speed. Experiments with

Manuscript received July 18, 1997; revised October 14, 1997. This work was suppoprted by the RACE Project 2039 ATMOS and the ACTS Project KEOPS and Project OPEN.

C. Joergensen, S. L. Danielsen, K. E. Stubkjaer, P. B. Hansen, H. N. Poulsen, A. Kloch, M. Vaa, and B. Mikkelsen are with the Center for Broadband Telecommunications, Department of Electromagnetic Systems, Technical University of Denmark, DK-2800 Lyngby, Denmark.

M. Schilling, K. Daub, E. Lach, G. Laube, W. Idler, and K. Wunstel are with Alcatel Telecom Research Division, Stuttgart, Alcatel Telecom, Department ZFZ/WO, D-70435 Stuttgart, Germany.

P. Doussiere and F. Pommerau are with Alcatel Alsthom Recherche, F-91460 Marcoussis, France.

Publisher Item Identifier S 1077-260X(97)09175-2.

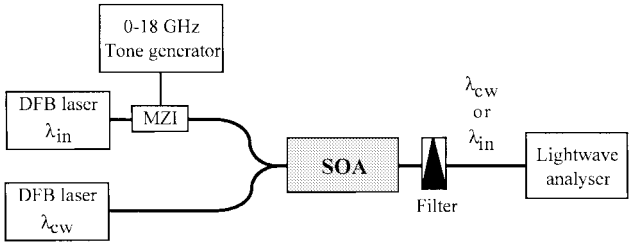

Fig. 1. Experimental setup for measuring the small-signal modulation bandwidth of XGM in SOA's.

XGM SOA wavelength converters operating at up to 40 Gb/s are described in Section III. The use of XPM requires the SOA's to be situated in an interferometric structure for conversion to intensity modulated signal formats. During the last couple of years there has been fast progress in the realization of monolithically integrated interferometric wavelength converters with SOA's in the arms of either Michelson (MI) or Mach–Zehnder interferometric (MZI) structures. High-speed interferometric wavelength converters are described in Sections IV and V. Sections VI and VII address the difference in optical modulation bandwidth encountered between the co- and counterdirectional coupling schemes and between the MI and MZI wavelength converters, respectively. Finally, the summary is given in Section VIII.

II. Small-Signal Modulation Bandwidth of SOAS

The speed capability of SOA-based converters can be assessed by optical small-signal modulation of the gain. This section presents an experimental and theoretical investigation of the modulation response.

Experimentally the setup in Fig. 1 is applied. It uses a small signal at wavelength λ_{in} that is modulated by a frequency swept sinusoidal. The induced modulation on the CW light at λ_{cw} (that is coupled to the SOA together with the signal) is analyzed at the SOA output using a lightwave analyzer. As an example, Fig. 2 gives the relative AM responses for the output signals at λ_{in} and λ, respectively, using a M-DCPBH SOA [44]. The converted signal exhibits a low-pass characteristic with a 3-dB modulation bandwidth of ~12 GHz while the amplified input signal clearly exhibits a high-pass filter characteristic. As recognized previously, this high-pass filtering of the input signal is important for the high conversion speeds that can be achieved [45]. For clarity, we will briefly recapitulate the analysis that accounts for the longitudinal evolution of the input signal and the continuous-wave (CW) light as they travel through the amplifier:

Traditionally, the effective carrier lifetime τ_e in the active waveguide is the parameter that determines the modulation bandwidth. For a very short amplifier the carrier density modulation, ΔN, caused by small-signal modulation of the optical input photon density, ΔS_{in}, at the frequency f_{mod} is given by [46]

$$\Delta N(f_{\text{mod}}) = -g_m \Delta S_{\text{in}}(f_{\text{mod}}) v_g \frac{\tau_e}{1 + j2\pi f_{\text{mod}} \tau_e} \qquad (1)$$

where g_m and v_g is the material gain and the group velocity, respectively. Hence, the carrier modulation response exhibits

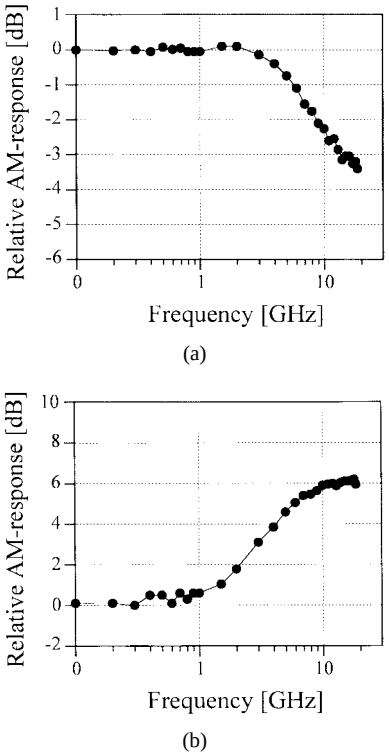

Fig. 2. Measured small-signal AM-response for both (a) input and (b) converted signal using a 1000-μm-long M-DCPBH SOA. Bias current: 150 mA. Input signal wavelength: 1560 nm. CW light wavelength: 1550 nm.

the well-known low-pass characteristic with an optical 3-dB bandwidth of $\sqrt{3/(2\pi\tau_e)}$. τ_e is the effective carrier lifetime given by [47]

$$\frac{1}{\tau_e} = \frac{dR_{\text{sp}}}{dN} + \frac{d}{dN}(g_m S v_g) \qquad (2)$$

where dR_{sp}/dN is the reciprocal differential carrier lifetime and the second term accounts for the speed-up associated with stimulated recombinations. Fig. 3(a) gives the calculated effective carrier lifetime versus the position in the SOA for different injection currents. The results are based on (2) combined with a detailed numerical SOA model that gives the carrier density as well as the optical fields along the SOA cavity [47], [45]. We observe that the effective carrier lifetime decreases with injection current since both terms in (2) increases. Moreover, for 200-mA injection current the effective carrier lifetime becomes as low as ~40 ps at the rear part of the SOA because the input signals are amplified through the SOA thereby increasing the stimulated recombination rate. The corresponding optical 3-dB modulation bandwidth is ~7 GHz, which is much lower than the ~20 GHz obtained from the numerical model as seen in Fig. 3(b). The reason for this discrepancy is that the relation between the effective carrier lifetime and the modulation bandwidth is valid only locally. To get the total modulation response of the SOA the longitudinal evolution of the optical signals must be taken into account. If we divide the amplifier into small sections, the output signal modulation, ΔS_{out}, from a given SOA section with length L

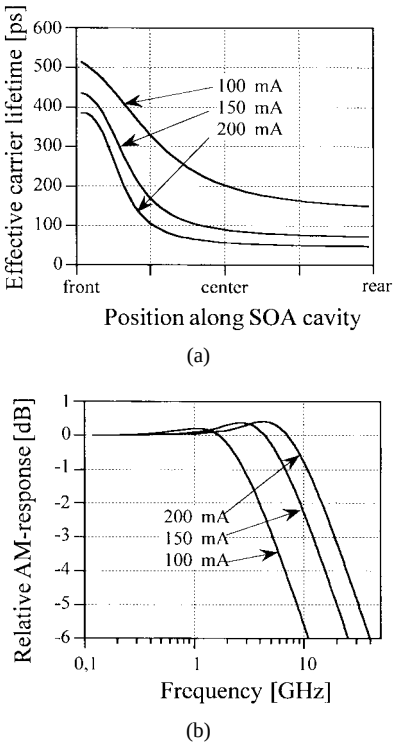

Fig. 3. (a) Calculated effective carrier lifetime versus the longitudinal position in the SOA cavity. (b) Calculated relative response versus modulation frequency for different bias currents. SOA length: 1200 μm. Input signal wavelength 1570 nm, CW light wavelength: 1550 nm. Input signal power: -7 dBm, CW power: -8 dBm. Codirectional coupling scheme.

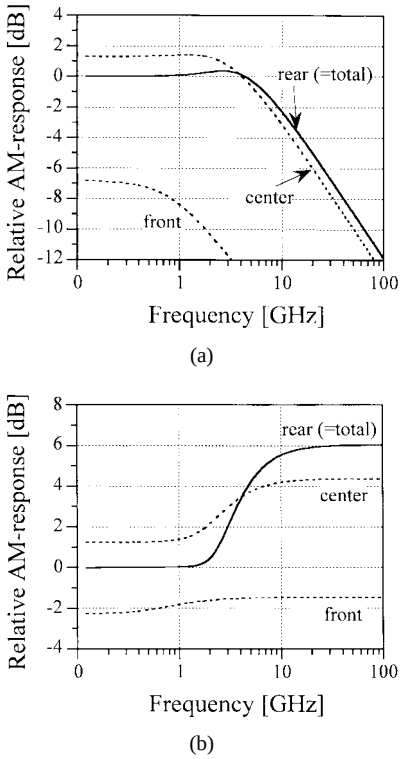

Fig. 4. Calculated relative AM response for (a) converted signal and (b) amplified input signal after different sections of the SOA converter. Solid curves give the total responses. SOA length: 800 μm. Input signal wavelength 1570 nm, CW light wavelength: 1550 nm. Input signal power: -7 dBm, CW light power: -8 dBm. Bias current density: 25 kA/cm^2. Codirectional coupling scheme.

and an input modulation, ΔS_{in}, is given by [45]

$$\Delta S_{\text{out}}(f_{\text{mod}}) = \Delta S_{\text{in}}(f_{\text{mod}})G + \Gamma \frac{dg_m}{dN} L S_{\text{in}} \Delta N(f_{\text{mod}}) \tag{3}$$

where S_{in} is the average input photon density, G is the single pass gain of the section, and Γ is the optical confinement factor. Comparing with (1), we see that the low pass characteristic of ΔN is subtracted from the signal modulation. This is the case in every section of the SOA thus emphasizing the high-frequency content of the input signal giving the high-pass filtering of the signal as observed experimentally in Fig. 2(b). Consequently, the input signals high-frequency components are amplified as it traverses the SOA thus equalizing the resulting modulation of the CW light. So, the low frequency content of the input signal is mainly transferred to the CW light in the front part of the SOA, whereas, the high-frequency content mainly is transferred in the rear part. This is clearly seen from Fig. 4 that gives the calculated responses for the converted signal and the input signal in the front, center and rear parts of the SOA. It is noticed that the rear part responses are resembling the measurements in Fig. 2. The predictions of the numerical model have been verified from comparison with experimental results as shown in [45].

The numerical modeling leads to simple guidelines for achieving high modulation bandwidth. The SOA's must be operated with:

1) large current injection and
2) high optical power levels.

Moreover, the SOA waveguides should have:

3) large optical confinement factors and
4) large differential gain.

Following these guidelines, work toward high-speed converters has been carried out. The wish for a high injection current translates into using SOA's with a long cavity since the maximum current density for the structures is $\sim$25–30 kA/cm^2. This was verified in experiments for otherwise identical SOA's with cavity lengths of 450, 800, and 1200 μm. Operated with the same injection currents the different SOA's had identical 3-dB modulation bandwidths of $\sim$17 GHz irrespective of cavity length. When operated at identical current densities of 25 kA/cm^2 they had modulation bandwidths of 7, 17, and 20 GHz, respectively.

In Fig. 5(a), the responses of even longer SOA's are studied. As seen small-signal modulation bandwidths as high as $\sim$90 GHz are predicted for a 3600-μm-long SOA. It should be noted, however, that even though long SOA's have large modulation bandwidths for the conversion they also have some disadvantages.

- Because of the large transit time of long SOA's, only copropagation of the input signal and the CW light can be used since the counterdirectional coupling scheme has speed limitations as discussed in Section VI.
- The spectral bandwidth shrinks as the cavity length increases.
- Very long SOA's with uniform cross sections of the active region are generally difficult to fabricate.

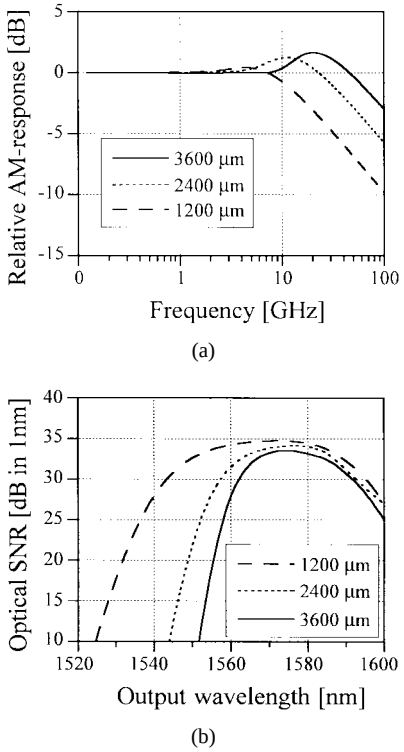

Fig. 5. Calculated AM-response (a) and optical SNR versus output wavelength (b) for cavity lengths of 1200, 2400, and 3600 μm. Input signal wavelength: 1570 nm, CW light wavelength: 1550 nm. Input signal power: -7 dBm, CW light power: -8 dBm. Current density: 25 kA/cm^2. Codirectional coupling scheme.

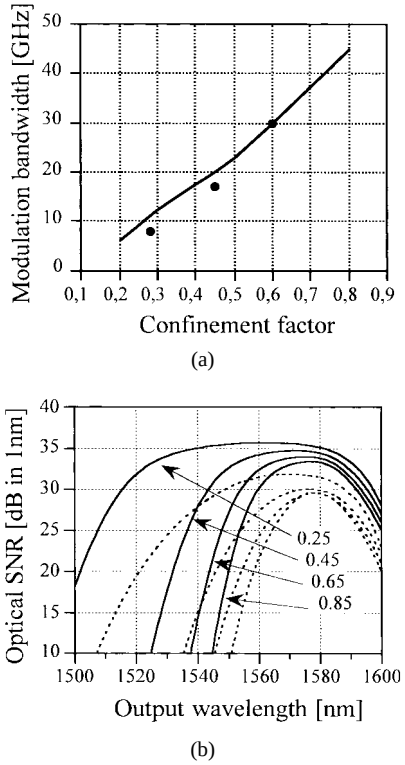

Fig. 6. (a) Measured and calculated 3-dB modulation bandwidths versus the confinement factor. (b) The optical signal-to-noise ratio versus output wavelength with the confinement factor as parameter for both codirectional coupling (solid lines) and counterdirectional coupling (dashed lines). SOA length: 1200 μm. Input signal wavelength: 1570 nm, CW light wavelength: 1550 nm. Input signal power: -7 dBm, CW light power: -8 dBm. Current density: 25 kA/cm^2.

The reduced spectral bandwidth is also illustrated in Fig. 5(b) that gives the optical signal-to-noise ratio (OSNR) versus the output signal wavelength (in 1-nm bandwidth). The spectral bandwidth, defined by an OSNR of 30 dB is decreased from 50 to 25 nm when the SOA length increases from 1200 to 3600 μm. This spectral bandwidth shrinkage for long SOA's is the same as observed when filters or amplifiers with nonflat transfer characteristic are concatenated.

Since the use of long amplifiers for increased modulation bandwidth for the conversion has some shortcomings as discussed above, focus has also been on developing SOA's with a large optical confinement factor. As mentioned in the guidelines above and as can be seen from (1) and (3), an increased optical confinement factor will increase the conversion modulation bandwidth. The theoretical estimates given by the full line in Fig. 6(a) show that by increasing the confinement factor from 0.2 to 0.8 the modulation bandwidth is increased by a factor of 9, i.e., from 5 to 45 GHz. The theoretical predictions are confirmed by the experiments shown by filled circles (note that the 3-dB conversion modulation bandwidth for a confinement factor of 0.6 is extrapolated from the transfer function in Fig. 7). As is the case for increased cavity length, an increased confinement factor also leads to a smaller spectral bandwidth. This is seen from Fig. 6(b) where solid and dashed lines are for co- and counterdirectional coupling of input and CW light in the SOA converter. The case of counterdirectional coupling will be commented more in detail in Section VI. For codirectional coupling it is seen that a confinement factor of 0.85 results in a spectral bandwidth of only 30 nm (at an OSNR

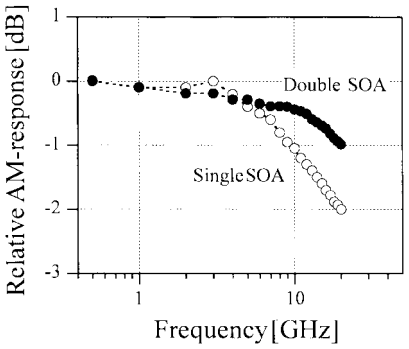

Fig. 7. Measured relative AM-response for conversion from 1554 nm (input power: 5 dBm) to 1548 nm (CW light power: 5 dBm) for single and double SOA converter. Bias current to each SOA: 300 mA. Codirectional coupling scheme. Optical confinement factor: 0.6.

of 30 dB). It should be emphasized, that in the SOA design, the optimum choice between spectral optical bandwidth and conversion modulation bandwidth is dependent on the specific application.

The fourth guideline prescribes a high differential gain, dg/dN, of the active waveguide material as may also be deducted from (2) and (3). Using quantum-well stacks, a higher differential gain can generally be obtained compared to bulk type material.

Following the considerations above, optimization of the 1200-μm-long SOA structure has been carried out thereby

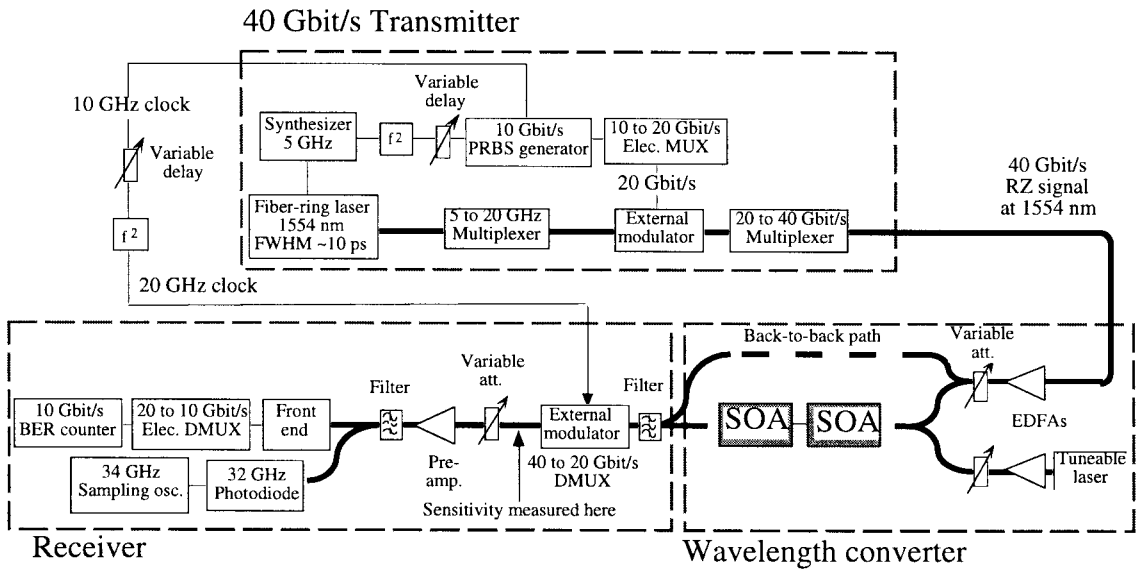

Fig. 8. Experimental setup for 40-Gb/s XGM wavelength conversion experiments.

increasing the confinement factor from 0.45 to 0.6. The optimized structures result in a large modulation bandwidth as shown in Fig. 7. For an injection current of 300 mA, a 3-dB modulation bandwidth of ~30 GHz is extrapolated using a single SOA. To simulate a long SOA cavity we use a simple concatenation of two 1200-μm-long SOA's that are connected directly by a short (20 cm) fiber cable without optical isolation or filtering. The losses of ~4 dB for the coupling in and out of the fiber will of cause influence the power levels and thereby the resulting modulation bandwidth compared to one long cavity, but the approach still allows assessment of the influence of a higher total injection current. For the concatenated SOA's, the total injection current is doubled to 600 mA leading to a much higher modulation bandwidth of ~50 GHz (extrapolated) as also indicated in Fig. 7. This bandwidth improvement is in qualitative agreement with similar experiments carried out in [48] as well as the predictions in Fig. 5(a). The speed advantages of a long SOA cavity are clear from the 40-Gb/s XGM system experiments reported in the next section.

III. BER Assessment of a 40-Gb/s XGM Wavelength Converter

The ultimate test of high-speed wavelength converters is obtained by bit-error-rate assessment. The setup in Fig. 8 was constructed for 40-Gb/s wavelength conversion with the optimized SOA structures described in the previous section. Short pulses generated by a fiber-ring laser are multiplexed in fiber delay line multiplexers to 20 GHz before modulation by a 20-Gb/s pseudorandom bit sequence (PRBS) sequence using an external modulator. Optical multiplexing is then used to form a 40-Gb/s signal at 1554 nm. This is coupled to the wavelength converter together with the CW light at the desired output wavelength. At the output, the converted signal is selected by an optical filter followed by optical demultiplexing to 20 Gb/s using a MZI modulator driven by a 20–GHz electrical tone. Subsequently we use electrical demultiplexing to 10 Gb/s before error counting. The converter is either a single SOA or two SOA's in cascade for high-speed operation as described in the previous section.

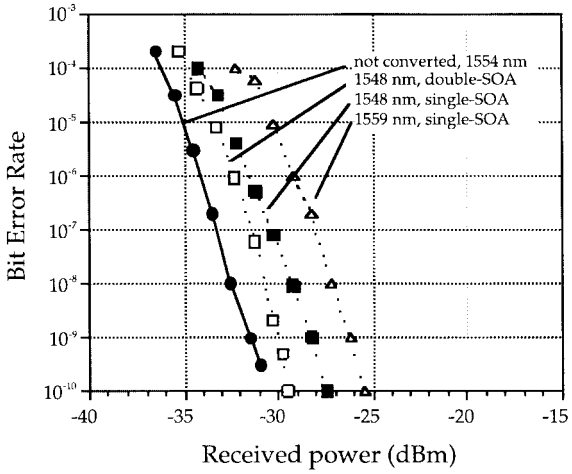

Fig. 9. Measured BER for 40-Gb/s XGM wavelength conversion using a single or two cascaded SOA's. Input signal power at 1554 nm is 5.5 dBm for conversion to 1548 nm (single and double SOA configurations) and 7.5 dBm for conversion to 1559 nm (single SOA only). The CW light power is ~4 dBm. Power levels are referred to the fiber before coupling. Eye-diagrams for the considered cases are shown in Fig. 10.

Fig. 9 gives the BER versus the received power (measured before the optical preamplifier) using both a single and a double SOA converter. For the single SOA converter operated at relatively high optical power levels of ~5 dBm (measured in the fiber) the penalty is 5.5 dB for conversion from 1554 to 1559 nm while a penalty of 3.5 dB is observed for conversion from 1554 to 1548 nm. The penalty difference is explained by the lower differential gain experienced by the CW light when its wavelength is longer than that of the input signal [49]. This is also evident from the measured eye-diagrams in Fig. 10(a)–(c) for the input signals and the two converted signals. The conversion to longer wavelength [Fig. 10(b)] results in a low extinction ratio of 7 dB, whereas, the extinction ratio for conversion to the shorter wavelength

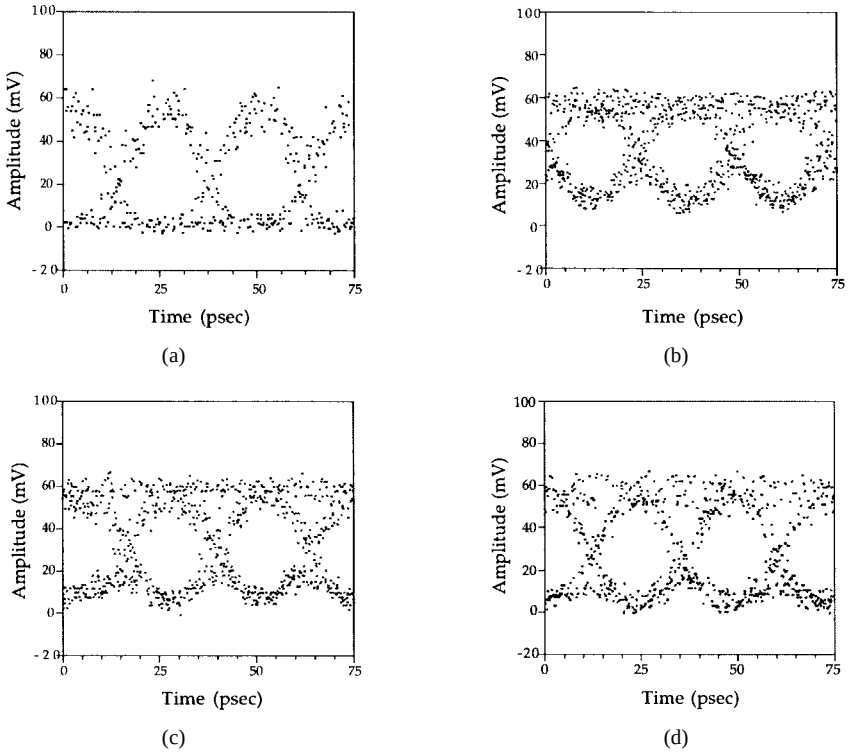

Fig. 10. (a) 40-Gb/s eye-diagrams for input signal at 1554 nm; (b) for converted signals at 1559 nm and (c) 1548 nm, using a single XGM SOA wavelength converter; and (d) converted signal at 1548 nm using two cascaded SOA's for the converter.

[Fig. 10(c)] is 9 dB. It should be noted that due to the limited modulation bandwidths of detector and oscilloscope, the pulses are broadened to NRZ-like waveforms.

For the double SOA converter with two times higher bias current the small-signal modulation bandwidth is increased as already seen in Fig. 7. The resulting performance improvement of the double SOA converter is clear from the BER curve in Fig. 9 for conversion from 1554 to 1548 nm. As seen, the penalty is decreased to only 1.5 dB corresponding to a 2-dB improvement compared to a single SOA. From the eye diagram in Fig. 10(d) for the double SOA configuration we observe an output extinction ratio of ~11 dB. From comparison of the eye-diagrams it is also evident that the longer wavelength converter has a much faster dynamics.

In addition to the low penalties it should be noted, that the converters with their output powers of ~6 dBm have no fiber-to-fiber losses. Moreover, the optical SNR is as high as 30 dB (measured in 1-nm spectral bandwidth) for the converted signals. These features enable cascading of several converters as will be required in meshed optical networks with many nodes.

IV. Interferometric Wavelength Converters

The low extinction ratio for conversion to longer wavelengths using XGM wavelength converters combined with a relatively high chirp for the converted signal has led to development of wavelength converters that use XPM in SOA's. In these converters the cross phase modulation is translated into an intensity modulation by placing the SOA's in the arms of interferometers typically with MZI or MI configuration [31]–[36], [42], [50]–[54]. SOA's are preferred to optical fiber as the nonlinear element due to the higher nonlinear refractive index and the compact and stable devices that result.

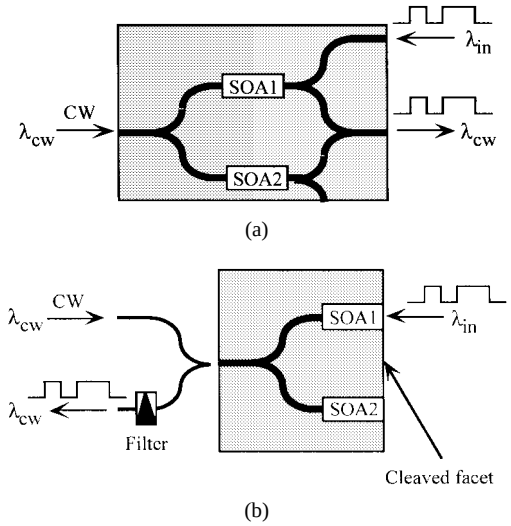

Fig. 11. Schematic of interferometric wavelength converters. (a) Symmetric MZI; (b) MI.

Progress in realization of monolithically integrated structures has been significant during the last two years. The MZ structures have been developed into structures with a separate waveguide for coupling the input signal into only one of the SOA's as shown in Fig. 11(a). The idea is that the input signal depletes the carrier concentration in only one of the SOA's thereby creating the wanted phase difference between the two interferometer arms in a very efficient way.

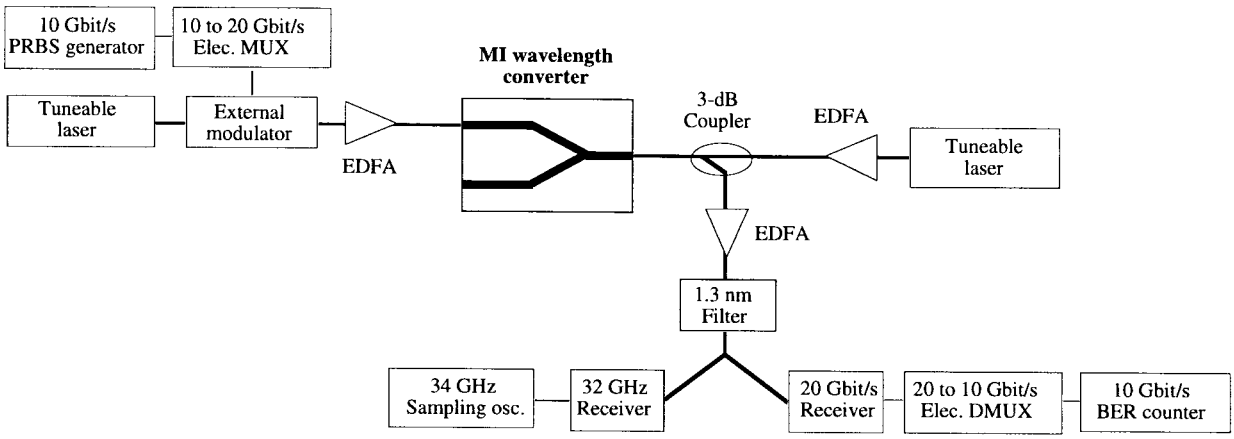

Fig. 12. Experimental setup for assessment of the BER performance at 20 Gb/s for the integrated MQW MI wavelength converter.

The MI converter in Fig. 11(b) has a reflective facet making it a folded version of the MZI converter. Therefore, it works very similarly. It should be noted, however, that the MZI allows the CW-light and the input signal to be launched counter-directionally, whereas, for the MI, a part of the original signal will always pass through the converter and be transmitted along with the converted signal. This prohibits the input and output wavelengths to be identical due to interference crosstalk. On the other hand, the MI allows the input signal to be coupled directly to one SOA without passing lossy couplers. The high optical power levels due to the direct coupling will enable a high modulation bandwidth, cf., the guidelines given in Section II.

The Sagnac interferometer that is very popular for time demultiplexing [55] can in principle also be used as a wavelength converter. The converter is inherently balanced, however, only RZ signals can be handled and the signal bit rate is determined by the placement of the SOA in the loop. Therefore, we will not consider the Sagnac interferometer further.

The MZI converter was first realized in an asymmetric version [50] that differs from the symmetric MZI in Fig. 11(a) by having only one optical input. So instead of feeding the input signal via a separate coupler, the input signal is coupled together with the CW light to both interferometer arms. The phase difference between the interferometer arms is obtained by employing asymmetric couplers so that the carrier density and thereby the phase is modulated differently in the two arms. Clearly, this operation principle with the input signal entering both SOA's complicates the adjustment and control of the interferometer. Nevertheless, fine performance has been obtained with this device structure [50].

V. MI Wavelength Converter Operating at Bit Rates of Up To 40 Gb/s

The first integrated interferometric converters were limited to bit rates of about 10 Gb/s due to a relatively low optical confinement factor and low optical power levels inside the structures caused by interface losses associated with the monolithic integration. By optimizing the waveguide structures, the interferometric converters have potential for operating at high bit rates as already explained.

In this section, an optimized all-active MI wavelength converter is used to achieve 20- and 40-Gb/s wavelength conversion. In the all-active approach the whole interferometer structure including couplers is realized using the same active waveguide structure. The different sections of the converter are therefore defined by the electrodes as opposed to the active-passive integration scheme where coupler sections are implemented using passive waveguides. The all-active approach has the advantage that losses in the structure can be counteracted by injecting current in the various converter sections. Furthermore, by using the MI rather than the MZI converter the input signal avoids the lossy coupler and waveguides.

The device [56] is realized using multiquantum-well based layer structures with a ten-well tensile strained InGaAs–InGaAsP waveguide core. This is an improvement relative to previous devices that had only five wells in the MQW stack and, therefore, a lower optical confinement factor. For lateral confinement a buried ridge stripe structure has been applied. The converter consists of an active 3-dB coupler followed by two 600-μm-long amplifier sections, resulting in a total device length of only 1.3 mm. The input port of the 3-dB coupler is anti-reflection coated and the gains in the different parts of the structure are determined by the bias currents applied to the electrodes.

A. BER Assessment of MI Wavelength Converter Operating at 20 Gb/s

The setup for assessing the BER performance of the MI converter at 20 Gb/s uses electrical multiplexing and demultiplexing between 10 and 20 Gb/s at the transmitter and receiver as shown in Fig. 12. The signal to be converted is generated by externally modulating a laser at 20 Gb/s by a MZI modulator. The signal is coupled directly to one of the amplifier sections of the MI structure (left facet in Fig. 12) thereby introducing a phase difference between the two arms. At the output the wavelength converted signal is selected by a 1.3-nm filter before error-counting and monitoring. Fig. 13 gives the recorded BER performance at 20 Gb/s. Negligible penalty is obtained using input power levels of 6 dBm (in the fiber) for both down (1560–1555 nm) and very importantly also up (1555–1560 nm) conversion. This demonstrates the

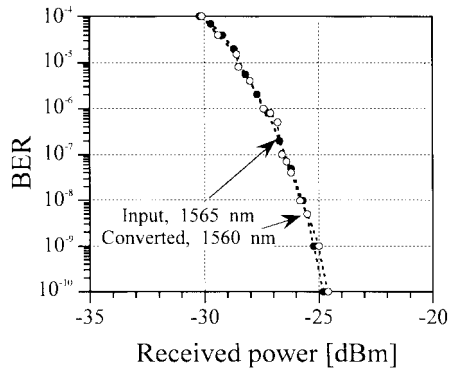

(a)

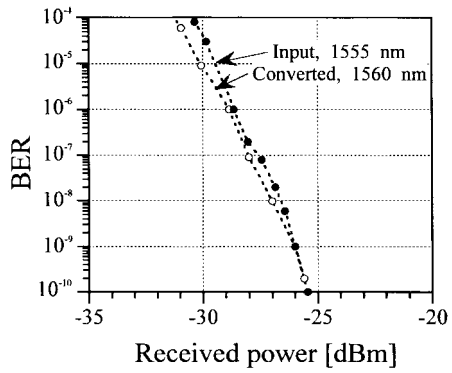

(b)

Fig. 13. Measured BER performance at 20 Gb/s for the input and converted signals using an all-active MI wavelength converter. Results are for conversion from 1565 to 1560 nm (a) and from 1555 to 1560 nm (b). Signal input power: 6 dBm. CW light power: 9 dBm.

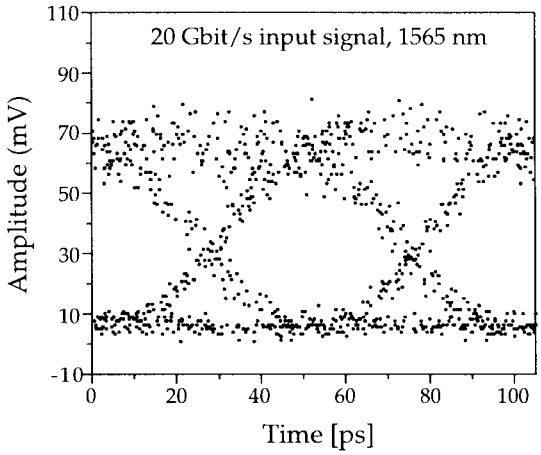

(a)

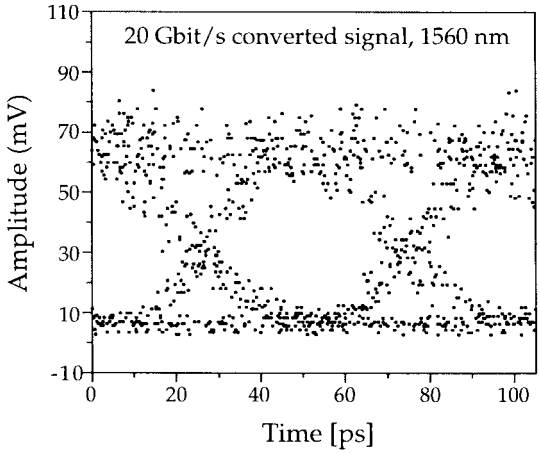

(b)

Fig. 14. Examples of eye-diagrams for input (a) and converted (b) signals at 20 Gb/s using the all-active MI wavelength converter.

very efficient wavelength conversion even at this high bit rate. The fine high-speed dynamics are also clear from the eye diagrams for input and output signals as shown in Fig. 14. The rising and falling edges of the 20 Gb/s converted signal are very similar to those of the input signal.

B. 40-Gb/s Experiments Using an MI Wavelength Converter

To assess the performance of the MI-converter at even higher bit rates, a 40-Gb/s system experiment has been performed. A 40-Gb/s RZ input signal is realized by first generating a train of short pulses with a gain-switched DFB laser. This is followed by delay-line multiplexers to achieve a 20-GHz pulse train that is encoded into a 20-Gb/s RZ signal with an external modulator. Afterwards the 40-Gb/s signal is realized using an additional delay line multiplexer. The setup is almost similar to that of Fig. 12 with the exception that we use a pulsed source to generate the input signal and that an additional delay line multiplexer is used to obtain the 40-Gb/s signal from the 20-Gb/s PRBS signal. At the converter output an optical circulator and a tuneable filter select the converted signal.

Fig. 15 illustrates the capability of the converter at 40 Gb/s by showing an eye diagram and a pulse trace for the conversion from 1559 to 1562 nm (up conversion). The extinction ratio of $\sim$10 dB clearly demonstrates the fine performance of the converter. Additionally, it should be mentioned that the optical signal-to-noise ratio is as high as 27 dB in 1-nm bandwidth.

The wavelength sensitivity is analyzed in Fig. 16 that gives the extinction ratio for the 40-Gb/s converted signals versus the output wavelength. Clearly, efficient up and down conversion is achieved with $\sim$10-dB extinction ratio. Moreover, the optical SNR is more than 25 dB (1 nm) for all wavelengths.

VI. Comparison of Coupling Schemes for the CW and Input Signal

The small-signal modulation bandwidths presented in Section II have all been for codirectional coupling of the CW and input signal to the SOA's. However, the counterdirectional coupling of the CW light and the input signal is more advantageous from a systems point of view, since it does not require an output filter to select the converted signal. Moreover, it allows for input and output wavelengths to be identical. In this section, the modulation bandwidth for the counterdirectional coupling scheme is compared to that for the codirectional coupling scheme.

Fig. 17 shows the relative response for the counterdirectional coupling scheme with the SOA cavity length as a parameter. The plot can be directly compared to the results for the codirectional coupling scheme in Fig. 5(a). For cavity lengths of up to 1200 μm the modulation bandwidths for

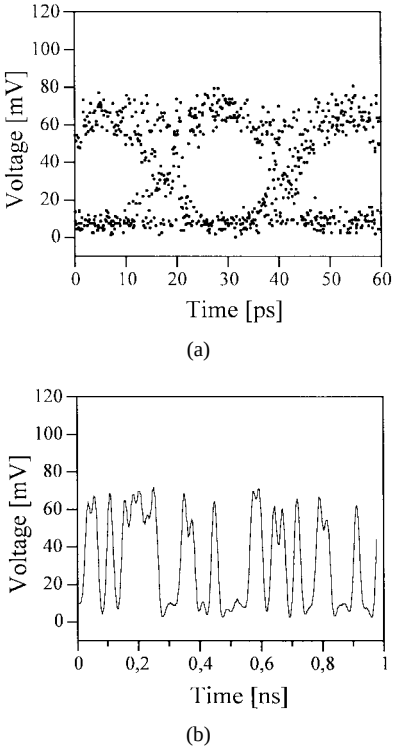

Fig. 15. (a) Measured eye-diagram and (b) waveform for 40-Gb/s converted signal using the all-active MI wavelength converter. Optical SNR (in 1 nm) is 27 dB. Signal input power at 1559 nm: 8 dBm. CW light power at 1562 nm: 9 dBm.

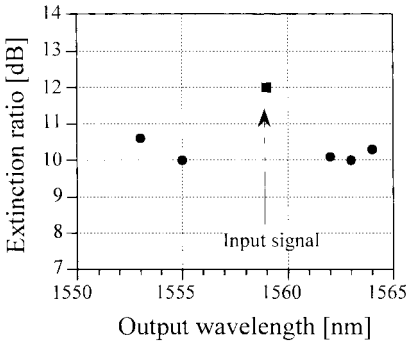

Fig. 16. Extinction ratios of converted 40-Gb/s signals versus the output wavelength using the all-active MI wavelength converter. Optical signal-to-noise ratios for all converted signals are >25 dB (in 1 nm).

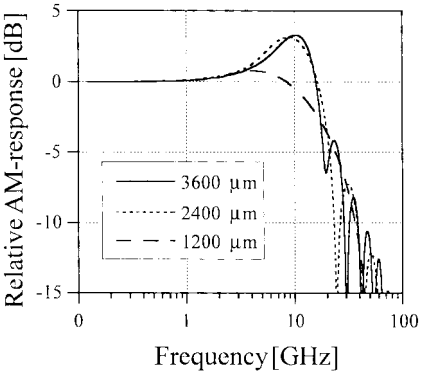

Fig. 17. Calculated AM response for the counterdirectional coupling scheme with the SOA cavity length as a parameter. Input signal wavelength 1570 nm, CW light wavelength: 1550 nm. Input signal power: −7 dBm. CW light power: −8 dBm. Current density: 25 kA/cm^2.

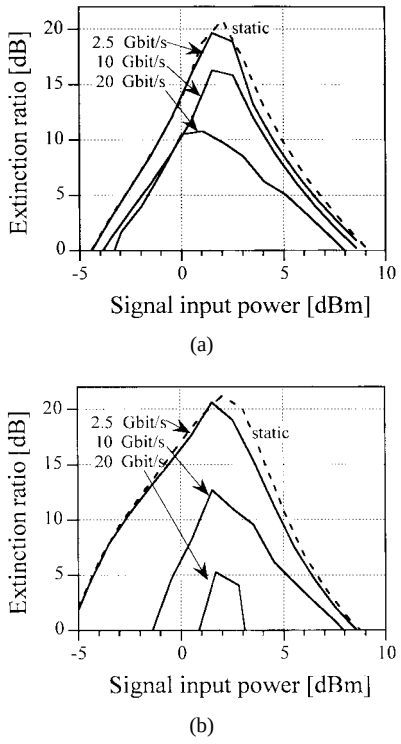

Fig. 18. Calculated static and dynamic extinction ratios versus signal input power for the codirectional (a) and the counterdirectional (b) coupling schemes using a symmetric MZI wavelength converter with 2400-μm-long SOA's. Conversion is from 1550 to 1560 nm. CW light power: −5 dBm. Current density: 25 kA/cm^2.

the co- and counterdirectional coupling schemes are almost identical. However, for longer SOA's the transit time becomes significant resulting in an upper limit for the modulation bandwidth. The effect of the transit time is also apparent from the larger overshoot observed in Fig. 17 as well as from the oscillating response at high frequencies that occur because the saturation and therefore the carrier depletion is shifting along the cavity as the input signal shifts between high- and low-power levels. This effect contributes to jitter on the converted signal.

For long SOA's the difference between the two coupling schemes is also clear from the large signal calculations in Fig. 18. Here, the extinction ratio for the converted signal versus input power is calculated for both static and dynamic cases assuming that 2400-μm-long SOA's are inserted into a symmetric MZI wavelength converter [see Fig. 11(a)]. The gains of the SOA's are adjusted to give almost identical static performance for the two coupling schemes. At low bit rate the extinction ratio follows the static curves for both co- and counterdirectional coupling. However, for increasing bit rates the performance for the counterdirectional coupling scheme deteriorates compared to the codirectional scheme due to the difference in dynamics as described above. For example, at 20 Gb/s, an extinction ratio above 10 dB can be obtained using the codirectional coupling scheme, whereas, only ∼5 dB extinction ratio is possible for counterdirectional coupling.

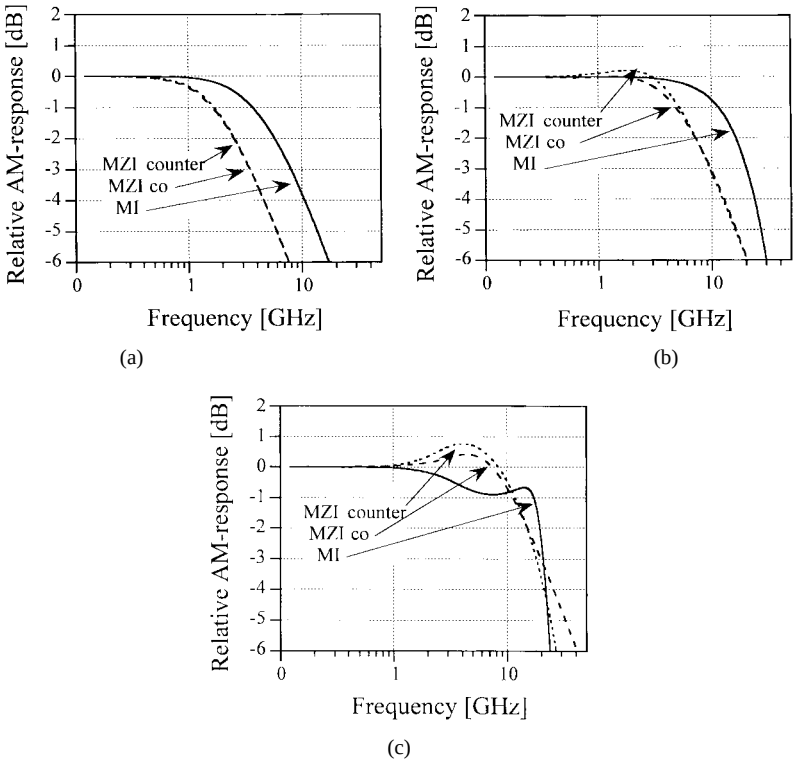

Fig. 19. Calculated AM response for MI and MZI wavelength converters with 300- (a), 600- (b) and 1200-μm long (c) SOA sections. Input signal wavelength: 1570 nm. CW light wavelength: 1550 nm. Input signal power: -7 dBm, CW light power: -8 dBm. Current density: 25 kA/cm^2.

Consequently, at high bit rates the input power dynamic range will generally be smaller when the counterdirectional coupling is employed.

It should be noted that in addition to the poorer dynamics, the counterdirectional coupling also suffers from a lower optical signal-to-noise ratio at the output compared to the codirectional scheme as illustrated by the dashed lines in Fig. 6(b). This is because the carrier density will be lower in the part of the SOA where the CW light enters since the amplified input signal that comes from the opposite direction causes a strong saturation.

VII. Modulation Speed of MZI and MI Wavelength Converters

In Section V, a MI wavelength converter is used for wavelength conversion at 40 Gb/s. In this section, we compare the modulation bandwidths of MI and MZI converters.

Fig. 19 shows the relative AM responses for MI and MZI wavelength converters with 300-, 600-, and 1200-μm-long SOA-sections. The converters are compared under equal conditions, i.e., the bias current and optical power levels coupled to the SOA's are identical for the two types of interferometers. For the MZI converter both the co- and counterdirectional coupling schemes are considered. Clearly, for a fixed SOA length the MI converter is much faster than the MZI converter. As an example, for 300-μm-long SOA-sections the modulation bandwidth is only $\sim$4 GHz for the MZI converter but $\sim$9 GHz for the MI converter. For 600-μm-long SOA sections, the corresponding improvement is from 10 to20 GHz. This is because the converted signal traverses the SOA twice in the MI converter due to the reflective facet. So the modulation bandwidth of the MI using SOA's of length L, effectively resembles that of a MZI using SOA's of length $2L$. This is verified from the calculations for the MI and MZI structures with 300- and 600-μm-long SOA sections, cf. Fig. 19(a) and (b). For even longer SOA sections the performance of the MI converter deteriorates as illustrated in Fig. 19(c). This is due to the long transit time experienced by the converted signal. Consequently, the highest bit-rate is obtained using the MZI converter with the codirectional coupling scheme.

VIII. Summary

In this paper, the modulation bandwidth of optically modulated SOA's used for XGM and XPM wavelength conversion has been investigated both experimentally and theoretically.

It has been verified that high-pass saturation filtering of the input signal as it traverses the SOA equalizes the total carrier modulation response experienced by the CW light. Therefore, the modulation bandwidth of the converters is much higher than predicted from the traditionally used effective carrier lifetime. The modulation bandwidth increases with the optical power levels, the total injected bias current, the confinement factor as well as the differential gain. Long SOA's are, therefore, preferred since they allow a high current injection. For XGM conversion with SOA's optimized according to these guidelines, we have shown experimental evidence for a $\sim$50-GHz bandwidth using two 1200-μm-long SOA's in cascade, each having a large confinement factor of 0.6. The drawback of long amplifiers with high confinement factors is the small wavelength range for high optical SNR's. Furthermore, the

calculations suggest that amplifiers longer than $\sim$1200 μm are not suitable for counterdirectional coupling of the signal and CW light because of a long SOA transit time.

The large converter modulation bandwidths have been exploited to carry out wavelength conversion experiments at bit rates up to 40 Gb/s. Polarization independent XGM conversion in two concatenated SOA's with high confinement factors resulted in penalties as low as $\sim$2 dB (preamplified receiver). Additionally, negligible conversion penalty for both up and down conversion has been demonstrated by an optimized and compact 1.3-mm-long all-active MQW MI structure at 20 Gb/s. Moreover, experiments at 40 Gb/s using the MI wavelength converter demonstrated high-quality converted signals with $>$10 dB extinction ratio and $>$25 dB optical SNR (in 1 nm).

Theoretical studies show that the MI converter is generally faster than the MZI converter due to the reflective facet in the MI configuration that allows the converted signal to transverse the SOA twice and moreover allows for direct coupling of the input signal into the amplifier sections. In case of very long SOA-sections the transit time may, however, cause speed limitations for the MI configuration. The issue of co- and counterdirectional coupling has been assessed theoretically with respect to modulation bandwidth and extinction ratio of the simple XGM as well as the MZI converters. The copropagation scheme has the largest modulation bandwidth and extinction ratio, but will also require filtering to eliminate the input signal after the converter.

Especially the interferometric converters have shown excellent properties with respect to bit-rate capability and signal quality for the converted signal. For practical applications the future challenge will be the development of packaged versions that are easily controlled.

ACKNOWLEDGMENT

The authors thank Dr. S. Bouchoule and her colleagues of CNET Bagneux for supply of gain switched DFB lasers for short pulse generation.

REFERENCES

[1] M. W. Chbat, A. Leclert, E. Jones, B. Mikkelsen, H. Février, K. Wünstel, N. Flaarønningen, J. Verbeke, M. Puleo, H. Melchior, P. Demester, J. Mørk, T. Olsen, and D. R. Hjelme, "The OPEN (Optical Pan-European Network) ACTS Project: early achievements and perspectives," in *Proc. of ECOC'96*, Oslo, Norway, Sept. 1996, vol. 4, paper WeP.11,.

[2] R. E. Wagner, R. C. Alferness, A. A. M. Saleh, and M. S. Goodman, "MONET: Multiwavelength optical metworking (invited paper)," *J. Lightwave Technol.*, vol. 14, pp. 1349–1355, June 1996.

[3] M. Berger, M. Chbat, P. Demeester, P. Godsvang, B. Hein, M. Huber, A. Jourdan, A. Leclert, R. Marz, T. Olsen, M. Sotom, G. Tobolka, B. Caenegem, and T. Broeck, "Pan-European optical networking using wavelength division multiplexing," *.IEEE Commun. Mag.*, vol. 35, no. 4, pp. 82–89, 1997.

[4] K. Sato, S. Okamoto, and H. Hadama, "Network performance and integrity enhancement with optical path layer technologies," *J. Select. Areas Commun.*, vol. 12, pp. 159–170, Jan. 1994.

[5] S. J. B. Yoo, "Wavelength conversion technologies for WDM network applications," *J. Lightwave Technol.*, vol. 14, pp. 955–966, June 1996.

[6] P. A. Perrier *et al.*, "Rack-mounted optical add/drop multiplexers in a self-healing multiwavelength ring network," in *Proc. Photonics in Switching*, Sendai, Japan, Apr. 1996, pp. 166–167.

[7] R. Schnabel, U. Hilbk, Th. Hermes, P. Meissner, Cv. Helmolt, K. Magari, F. Raub, W. Pieper, F. J. Westphal, R. Ludwig, L. Kuller, and H. G. Weber, "Polarization insensitive frequency conversion of a 10-channel OFDM signal using four-wave mixing in a semiconductor laser amplifier," *IEEE Photon. Technol. Lett.*, vol. 6, pp. 56–58, Jan. 1994.

[8] R. Ludwig and G. Raybon, "BER measurements of frequency converted signals using four-wave mixing in a semiconductor laser amplifier at 1, 2.5, 5, and 10 Gbit/s," *Electron. Lett.*, vol. 30, pp. 338–339, Jan. 1994.

[9] K. Inue, T. Hasegawa, and H. Toba, "Influence of stimulated Brillouin scattering on optimum lenght in fiber four-wave mixing wavelength conversion," *IEEE Photon. Technol. Lett.*, vol. 7, pp. 327–329, Mar. 1995.

[10] D. M. Patrick and R. J. Manning, "20 Gbit/s wavelength conversion using semiconductor nonlinearity," *Electron. Lett.*, vol. 30, pp. 252–253, Feb. 1994.

[11] E. Lach, D. Baums, K. Daub, T. Feeser, W. Idler, G. Laube, G. Luz, M. Schilling, and K. Wünstel, "5 Gbit/s wavelength conversion with simultaneous regeneration of extinction ratio using Y-lasers," in *Proc. ECOC'93*, Montreux, Switzerland, Sept. 1993, vol. 2, pp. 137–140.

[12] K. Weich, J. Hörer, E. Patzak, D. J. As, R. Eggemann, and M. Möhrle, "Injection locked laser as wavelength converter and optical regenerator up to 10 Gbit/s," in *Proc. ECOC '94*, Firenze, Italy, Sept. 1994, vol. 2, pp. 643–646.

[13] P. Pottier, M. J. Chawki, R. Auffret, G. Glaveau, and A. Tromeur, "1.5 Gbit/s transmission system using all optical wavelength converter based on tuneable two-electrode DFB-laser," *Electron. Lett.*, vol. 27, pp. 2183–2185, 1991.

[14] G.-H. Duan *et al.*, "1 Gbit/s operation of optically triggered MQW bistable lasers incorporating a proton bombarded absorber," in *Proc. CLEO'93*, Baltimore, May 1993, p. 416, paper CThH5.

[15] T. Durhuus, R. J. S. Pedersen, B. Mikkelsen, K. E. Stubkjaer, M. Öberg, and S. Nilsson, "Optical wavelength conversion over 18 nm at 2.5 Gbit/s by DBR laser," *IEEE Photon. Technol. Lett.*, vol. 5, pp. 86–88, Jan. 1993.

[16] R. J. S. Pedersen, B. Mikkelsen, T. Durhuus, C. Braagaard, C. Joergensen, K. E. Stubkjaer, M. Öberg, and S. Nilsson, "Simple wavelength conversion for bitrate independent operation up to 10 Gbit/s," in *Proc. OFC'94*, San Jose, CA, Feb. 1994, paper ThQ3.

[17] C. Caspar, H.-M. Foisel, E. Patzak, B. Strebel, and K. Weich, "Improvement of crosstalk tolerances in optical cross connects by regenerative frequency converters," in *Proc. ECOC'96*, Oslo, Norway, Sept. 1996, vol. 4, paper ThD.1.5.

[18] H. Sanjoh, H. Mawatari, H. Ishii, H. Yasaka, Y. Yoshikuni, and K. Oe, "Wavelength chirping in wavelength conversion of 10 Gbit/s signal with semiconductor laser converter," *IEEE Photon. Technol. Lett.*, vol. 8, pp. 296–298, Feb. 1996.

[19] K. Inoue, H. Takahashi, S. Suzuki, K. Oda, "Wavelength conversion using a light injected DFB-LD and a Mach-Zehnder filter with a ring resonator," *IEEE Photon. Technol. Lett.*, vol. 7, pp. 998–1000, Sept. 1995.

[20] T. Durhuus, B. Fernier, P. Garabedian, F. Leblond, J. L. Lafragette, B. Mikkelsen, C. G. Joergensen, and K. E. Stubkjaer, "High speed all-optical gating using two-section semiconductor optical amplifier structure," in *Proc. CLEO'92*, Anaheim, CA, 1992, paper CThS4.

[21] J. Mellis, "Direct optical phase modulation of semiconductor laser amplifier," *Electron. Lett.*, vol. 25, pp. 679–680, 1989.

[22] H. Izadpanah, A. Elrefaie, C. Lin, and A. Alhamdan, "Semiconductor optical amplifier as low chirp multi-Gb/s modulator with gain," in *Tech. Dig. OFC'90*, San Francisco, CA, Jan. 1990, paper PD34.

[23] B. Glance, J. M. Wiesenfeld, U. Koren, A. H. Gnauck, H. M. Presby, and A. Jourdan, "High performance optical wavelength shifter," *Electron. Lett.*, vol. 28, no. 18, pp. 1714–1715, Aug. 1992.

[24] J. M Wiesenfeld and B. Glance, "Cascadability and fanout of semiconductor optical amplifier wavelength shifter," *IEEE Photon. Technol. Lett.*, vol. 4, pp. 1168–1171, 1992.

[25] C. Joergensen, T. Durhuus, C. Braagaard, B. Mikkelsen, and K. E. Stubkjaer, "4 Gb/s optical wavelength conversion using semiconductor optical amplifiers" *IEEE Photon. Technol. Lett.*, vol. 5, pp. 657–660, June 1993.

[26] J. M. Wiesenfeld, B. Glance, J. S. Perino, and A. H. Gnauch, "Wavelength conversion at 10 Gb/s using a semiconductor optical amplfier," *IEEE Photon. Technol. Lett.*, vol. 5, pp. 1300–1303, Nov. 1993.

[27] I. Valiente, J. C. Simon, and M. Le Ligne, "Theoretical analysis of semiconductor optical wavelength shifter," *Electron. Lett.*, vol. 29, pp. 502–503, 1993

[28] B. Mikkelsen, M. Vaa, R. J. Pedersen, T. Durhuus, C. Joergensen, C. Braagaard, N. Storkfelt, K. E. Stubkjaer, P. Doussiere, G. Garabedian, C. Graver, E. Derouin, T. Fillion, and M. Klenk, "20 Gbit/s polarization insensitive wavelength conversion in semiconductor optical amplifiers," in *Proc. ECOC'93*, Montreux, Switzerland, Sept. 1993, vol. 3 pp. 73–76.

[29] J. M. Wiesenfeld, J. S. Perino, A. H. Gnauch, and B. Glance, "Bit error

rate performance for wavelength conversion at 20 Gb/s," *Electron. Lett.*, vol. 30, pp. 720–721, Apr. 1994.
[30] S. L. Danielsen, C. Joergensen, M. Vaa, B. Mikkelsen, K. E. Stubkjaer, P. Doussiere, F. Pommerau, L. Goldstein, R. Ngo, and M Goix, "Bit error assessment of 40 Git/s all-optical polarization independent wavelength converter," *Electron. Lett.*, vol. 32, pp. 1688–1689, Aug. 1996.
[31] C. Joergensen, T. Durhuus, B. Mikkelsen, and K. E. Stubkjaer, "Wavelength conversion at 2.5 Gbit/s using a Mach-Zehnder interferometer with SOA's," in *Proc. Optical Amplifiers and their Applications*, Yokohama, Japan, July 1993, paper MD2.
[32] T. Durhuus, C. Joergensen, B. Mikkelsen, R. J. S. Pedersen, and K. E. Stubkjaer, "All optical wavelength conversion by SOA's in a Mach–Zehnder configuration," *IEEE Photon. Technol. Lett.*, vol. 6, pp. 53–55, Jan. 1994
[33] M. Schilling, T. Durhuus, C. Joergensen, E. Lach, D. Baums, K. Daub, W. Idler, D. Laube, K. Stubkjaer, and K. Wünstel, "Monolithic Mach–Zehnder Interferometer based optical wavelength converter operated at 2.5 Gbit/s with extinction ratio improvement and low penalty," in *Proc. ECOC '94*, Firenze, Italy, Sept. 1994, vol. 2, pp. 647–650.
[34] N. Vodjdani, F. Ratovelomanana, A. Enard, G. Glastre, D. Rondi, R. Blondeau, T.Durhuus, C. Joergensen, B. Mikkelsen, and K. E. Stubkjaer, "All optical wavelength conversion with SOA's monolithically integrated in a passive Mach–Zehnder interferometer," in *Proc. ECOC'94*, Firenze, Italy, Sept. 1994, vol. 4, pp. 95–98.
[35] B. Mikkelsen, T. Durhuus, C. Joergensen, R. J. S. Pedersen, S. L. Danielsen, K. E. Stubkjaer, M. Gustavsson, W. van Berlo, and M. Janson, "10 Gbit/s wavelength converter realized by monolithic integration of semiconductor optical amplifiers and Michelson interferometer," in *Proc. ECOC'94*, Firenze, Italy, Sept. 1994, vol. 4, pp. 67–70.
[36] X. Pan, J. M. Wiesenfeld, J. S. Perino, T. L. Koch, G. Raybon, U. Koren, M. Chien, M. Young, B. I. Miller, and C. A. Burrus, "Dynamic operation of a three-port, integrated Mach-Zehnder wavelength converter," *IEEE Photon. Technol. Lett.*, vol. 7, pp. 995–997, Sept. 1995
[37] A. E. Willner and W. Shieh, "Optimal spectral and power parameters for all-optical wavelength shifting: Single stage, fanout, and cascadability," *J. Lightwave Technol.*, vol. 13, pp. 771–781, May 1995.
[38] C. Q. Xu, H. Okayama, and M. Kawahara, "Efficient broadband wavelength converter for WDM optical communication systems," in *Tech. Dig. OFC '94*, San Jose, CA, Feb. 1994, paper ThQ4.
[39] S. J. B. Yoo, C. Caneau, R. Bhat, and M. A. Koza, "Transparent wavelength conversion by difference frequency generation in AlGaAs waveguides," in *Tech. Dig. OFC'96*, San Jose, CA, Feb. 1996, paper WG7.
[40] N. Storkfelt, B. Mikkelsen, D. S. Olesen, M. Yamaguchi, and K. E. Stubkjaer, "Measurement of carrier lifetime and linewidth enhancement factor for 1.5-μm ridge-waveguide laser amplifier," *IEEE Photon. Technol. Lett.*, vol. 3, pp. 632–634, July 1991.
[41] C. Joergensen, S. L. Danielsen, P. B. Hansen, B. Mikkelsen, K. E. Stubkjaer, M. Schilling, K. Daub, E. Lach, G. Laube, W. Idler, and K. Wunstel, "Up to 20 Gbit/s bit-rate transparent integrated interferometric wavelength converter," in *Proc. ECOC'96*, Oslo, Norway, Sept. 1996, vol. 4, paper ThB.2.2.
[42] C. Joergensen, S. L. Danielsen, P. B. Hansen, K. E. Stubkjaer, M. Schilling, K. Daub, E. Lach, G. Laube, W. Idler, and K. Wunstel, "All-optical 40 Gbit/s compact integrated interferometric wavelength converters," In *Tech. Dig. OFC'97*, Dallas, TX, Feb. 1997, paper TuO1.
[43] J. Mark and J. Mørk, "Ultrafast gain dynamics in semiconductor amplifiers," in *Tech. Dig. Optical Amplifiers and their Applications Conf. '93*, Yokohama, Japan, July 1993, TuC1.
[44] P. Doussiere, P. Garabedian, C. Graver, B. Bonnevie, T. Fillion, E. Derouin, M. Monnot, J. G. Provost, D. Leclerc, and M. Klenk, "1.55 μm polarization independent semiconductor optical amplifier 25 dB fiber to fiber gain," *IEEE Photon. Technol. Lett.*, vol. 6, pp. 170–172, Feb. 1994.
[45] T. Durhuus, B. Mikkelsen, C. Joergensen, and K. E. Stubkjaer, "All optical wavelength conversion by semiconductor optical amplifiers," *J. Lightwave Technol.*, vol. 14, pp. 942–954, June 1996.
[46] T. Durhuus, "Semiconductor optical amplifiers: Amplification and signal processing," Ph.D. dissertation, Electromagnetics Inst., Technical Univ. of Denmark, Jan. 1994, publication no. LD 114.
[47] T. Durhuus, B. Mikkelsen, and K. E. Stubkjaer, "Detailed dynamic model for semiconductor optical amplifiers and their crosstalk and intermodulation distortion," *J. Lightwave Technol.*, vol. 10, pp. 1056–1065, Aug. 1992.
[48] D. D. Marcenac, A. E. Kelly, D. Nesset, and D. A. O. Davies, "Bandwidth enhancement of wavelength conversion via cross-gain modulation by optical amplifier cascade," *Electronics Letters*, vol. 31, pp. 1442–1443, Aug. 1995.
[49] K. E. Stubkjaer, T. Durhuus, B. Mikkelsen, C. Joergensen, R. J. Pedersen, C. Braagaard, M. Vaa, S. L. Danielsen, P. Doussiere, G. Garabedian, C. Graver, A. Jourdan, J. Jacquet, D. Leclerc, M. Erman, and M. Klenk, "Optical wavelength converters," in *Proc. ECOC '94*, Firenze, Italy, Sept. 1994, vol. 2, pp. 635–642.
[50] F. Ratovelomanana, N. Vodjdani, A. Enard, G.Glastre, D. Rondi, R. Blondeau, C. Joergensen, T.Durhuus, B. Mikkelsen, K. E. Stubkjaer, A. Jourdan, and G. Soulage, "An all-optical wavelength-converter with semiconductor optical amplifiers monolithically integrated in a asymmetric passive Mach–Zehnder interferometer," *IEEE Photon. Technol. Lett.*, vol. 7, pp. 992–994, Sept. 1995
[51] X. Pan and T. L. Koch, "Intensity noise characteristics of a Mach-Zehnder wavelength converter," *IEEE Photon. Technol. Lett.*, vol. 7, pp. 1276–1278, Nov. 1995.
[52] C. Joergensen, S.L. Danielsen, T. Durhuus, B. Mikkelsen, K.E. Stubkjaer, N. Vodjdani, F. Ratovelomanana, A. Enard, G. Glastre, D. Rondi, and R. Blondeau, "Wavelength conversion by optimized monolithic integrated Mach–Zehnder interferometer," *IEEE Photon. Technol. Lett.*, vol. 8, pp. 521–524, Apr. 1996.
[53] B. Mikkelsen, M. Vaa, N. Storkfelt, T. Durhuus, C. Joergensen, R. J. S. Pedersen, S. L. Danielsen, K. E. Stubkjaer, M. Gustavsson, W. van Berlo, and M. Janson, "Monolithic integrated Michelson interferometer with SOA's for high speed all-optical signal processing," in *Proc. OFC'95*, San Diego, CA, Feb. 1995, paper TuH4.
[54] F. Ratovelomanana, N. Vodjdani, A. Enard, G. Glastre, D. Rondi, R. Blondeau, and A. Jourdan, "Monolithic integration of Michelson all-optical wavelength converter," in *Tech. Dig. OFC'96*, San Jose, CA, Feb. 1996, paper WG3.
[55] E. Jahn, N. Agrawal, W. Pieper, H.-J. Ehrke, D. Franke, W. Fürst, and C.M. Weinert, "Monolithically integrated nonlinear Sagnac interferometer and its application as a 20 Gbit/s all-optical demultiplexer," *Electron. Lett.*, vol. 32, pp. 782–783, 1996.
[56] M. Schilling, W. Idler, G. Laube, K. Daub, K. Dütting, E. Lach, D. Baums, and K. Wünstel, "10 Gbit/s monolithic MQW-based wavelength converter in Michelson interferometer configuration," in *Tech. Dig. OFC'96*, San Jose, CA, Feb. 1996, paper WG2.

C. Joergensen, photograph and biography not available at the time of publication.

S. L. Danielsen, photograph and biography not available at the time of publication.

K. E. Stubkjaer (S'76–M'81), photograph and biography not available at the time of publication.

M. Schilling (M'90), photograph and biography not available at the time of publication.

K. Daub, photograph and biography not available at the time of publication.

P. Doussiere, photograph and biography not available at the time of publication.

F. Pommerau, photograph and biography not available at the time of publication.

P. B. Hansen, photograph and biography not available at the time of publication.

H. N. Poulsen, photograph and biography not available at the time of publication.

A. Kloch, photograph and biography not available at the time of publication.

M. Vaa, photograph and biography not available at the time of publication.

B. Mikkelsen, photograph and biography not available at the time of publication.

E. Lach, photograph and biography not available at the time of publication.

G. Laube, photograph and biography not available at the time of publication.

W. Idler, photograph and biography not available at the time of publication.

K. Wunstel, photograph and biography not available at the time of publication.